

**Technical Report 1664**  
June 1994

**Open Ocean Effectiveness of the  
Electro-Optical Tactical Decision Aid  
Mark III**

Charles P. McGrath

# EXECUTIVE SUMMARY

## OBJECTIVE

This report compares measured forward-looking infrared (FLIR) system detection ranges of a target ship, the Research Vessel *Point Sur*, with predictions from the Electro-Optical Tactical Decision Aid (EOTDA), version 3.0. The EOTDA was primarily developed by the Air Force, with only minimal attention applied to the complexities of the marine environment. The objective of this case study was to evaluate the infrared EOTDA performance for a target in an open ocean background.

## RESULTS

Surface meteorological and navigation data were recorded aboard the Research Vessel *Point Sur*. Eight FLIR missions were flown making 57 detection range measurements. The meteorological and navigation data were input to the EOTDA, and the prediction ranges were tabulated and compared with the reported FLIR data. Results showed reasonable accuracy during the clear-weather portion of the tests, but the EOTDA grossly overpredicted detection ranges when a stratus cloud ceiling prevailed. Attempts to determine integrated target temperature from thermistors mounted on the surface of the ship structure were unsuccessful. Since calibrated target and background temperatures were unavailable at the times of the FLIR detection range measurements, it was not possible to isolate the portion of the EOTDA most responsible for the overpredictions. However, the transmission model (LOWTRAN 7) is well-accepted in the scientific community, and the target model (TCM2) of the EOTDA performed well in another case study during the same field tests. This would make the water background model of the EOTDA most suspect.

## RECOMMENDATIONS

The cause of the overpredictions must be determined. Further investigation of the water, sky, and cloud radiance models of the EOTDA is recommended, especially in the marine environment. Future validations with FLIR systems should be accompanied with simultaneous measurements with a calibrated imaging system.

# CONTENTS

INTRODUCTION .....	1
BACKGROUND .....	1
EOTDA OVERVIEW .....	1
FLEET USE OF THE EOTDA .....	2
VALIDATION OF THE EOTDA .....	3
MEASUREMENTS .....	4
OVERVIEW OF FIELD TESTS .....	4
SHIPBOARD MEASUREMENTS .....	5
AIRBORNE PLATFORM MEASUREMENTS .....	5
AIRBORNE FLIR MEASUREMENTS .....	6
EOTDA OPERATION .....	6
RESULTS .....	6
DETECTION RANGES .....	6
BACKGROUND TEMPERATURES .....	7
TARGET TEMPERATURES .....	9
CONCLUSIONS .....	10
REFERENCES .....	11
APPENDICES:	
A. TABLES OF OBSERVED DETECTION RANGES AND EOTDA PREDICTIONS .....	13
B. TABLES OF MEASURED SEA TEMPERATURES AND EOTDA PREDICTIONS .....	17
C. BAR CHARTS OF OBSERVED AND PREDICTED DETECTION RANGES .....	21
<b>FIGURES</b>	
1. Research Vessel <i>Point Sur</i> GPS track .....	5
2. Observed detection ranges compared with EOTDA MDT range predictions .....	7
3. EOTDA calculated sea temperature compared with measured values .....	8
4. Background temperature differences over the test period (57 overflights); <i>Point Sur</i> thermistor values minus the EOTDA predicted values .....	8
5. Comparison of radiometric and physical sea temperatures .....	9
6. Emissivity and reflectance of sea water as a function of incidence angle .....	9
<b>TABLE</b>	
1. Comparison of target temperatures from the AGA-780 imager and the TDA predictions for the starboard and port sides .....	10

## INTRODUCTION

This report presents a set of airborne forward-looking infrared (FLIR) detection range data as a case study of the Electro-Optical Tactical Decision Aid (EOTDA) version 3.0. The EOTDA is a microcomputer code that predicts the performance of electro-optical systems applied to various targets for strike warfare missions. The EOTDA is currently being adapted to a workstation platform for inclusion into the Tactical Environmental Support System version 3.0 (TESS(3)) and the Tactical Aircraft Mission Planning System (TAMPS) version 6.0, under the direction of Naval Research Laboratory (NRL), Monterey, California.

The EOTDA supports three optical regions, the long-wave infrared (8–12  $\mu\text{m}$ ), visible (0.4–0.9  $\mu\text{m}$ ), and laser (1.06  $\mu\text{m}$ ). The scope of this report is limited to studying the infrared (8–12 m) range predictions for an airborne FLIR sensor directed toward a ship target against an open ocean background.

The detection ranges presented in this report were collected during field experiments conducted from 29 July to 4 August 1992 off the coast of Monterey, California. The purpose of the experiment was to collect meteorological and ship temperature data, infrared (IR) images, and airborne FLIR detection range data in support of ongoing research at the Naval Command, Control and Ocean Surveillance Center (NCCOSC), Research, Development, Test and Evaluation Division (NRaD) and the Naval Postgraduate School. The Research Vessel *Point Sur* was the meteorological measurement platform. Meteorological data collected onboard the *Point Sur* were converted to Terminal Aerodrome Forecast (TAF) code format for input into the EOTDA. The *Point Sur* was also used as the target for the FLIR and IR imaging systems.

The FLIR detection ranges were provided by aircrews who flew the missions in support of the field tests. Eight missions were flown, four at night and four during mid-morning, making a total of 57 passes at the target. The results from these overflights provide the primary foundation for this report.

## BACKGROUND

### EOTDA OVERVIEW

Strike warfare planning and vulnerability assessment relies on software-driven tactical decision aids (TDAs). The EOTDA Mark III (Freni, et al., 1993) was developed by the coordinated effort of several contractors and agencies, with Hughes STX Corporation bringing together the final product under the direction of the Air Force Phillips Laboratory. The EOTDA predicts the performance of a variety of sensors against a variety of user-defined targets and backgrounds. The sensors include long-wave IR, television, laser, and night-vision goggles (NVGs). The Navy, under the direction of NRL Monterey, leveraged upon the Air Force effort by adding Navy and Marine Corps sensors and targets to the already developed software. Sensors were added for several naval air platforms (e.g., A-6E, FA-18, P-3C, and F-14). Two ship targets (a frigate and a gunboat) have already been added, and a user-definable generic ship model developed by Georgia Technology Research Institute (GTRI) is currently being implemented.

IR sensor performance is greatly influenced by environmental conditions. The meteorological input parameters drive the outcome of the target, background, and atmospheric transmission

calculations. Unfortunately, compromises were made in the environmental and background models of the EOTDA. These compromises were necessary to afford reasonable computer run-times and to accommodate the intended operating platform, which was a personal computer with an 80286 microprocessor running under MS DOS. Therefore, a simplified two-layer version of LOWTRAN 7 (Kneizys, et al., 1988) determines the atmospheric transmittance, and the EOTDA target/background model employs the intermediate grade of TCM2 (Blakeslee and Rodriguez, 1993) instead of the more refined research grade software.

The target and background temperatures in the EOTDA are determined by the intermediate grade TCM2 model developed by Georgia Technology Research Institute. TCM2 is a first-principles thermal contrast model. It treats the target and background as a series of three-dimensional isothermal spatial nodes with specific material properties. After a steady-state initialization process, an energy balance solution using the laws of heat transfer are applied to the thermal network to determine the nodal heat transfers. Finally, the radiance values are calculated in the desired wave band for each node. The radiance values of the node facets that are visible in the field-of-view of the sensor are integrated to determine the overall target radiance. The intermediate grade TCM2 uses a one-dimensional solution and allows fewer nodes, thus limiting target resolution compared with the research grade TCM2. The background is modeled as a single homogeneous node resembling an isothermal plate surrounding the target, and the sky is considered a uniform hemisphere covering the target. The complexities of the background and sky, such as clutter, sea-surface wave-slope reflections, and diffuse scattering and cloud effects are ultimately combined into a homogenized background solution. The difference between the uniform background radiance and the integrated target radiance determines the zero-range thermal contrast. Whether this thermal contrast is representative of the real-world scene depends on many conditions, such as scene complexity and human recognition, and cueing factors.

The required meteorological inputs are entered in a user-friendly format. The user enters the surface and dewpoint temperatures graphically in 1° increments for the times of interest. From these temperatures, corresponding relative humidity values are calculated. Any of 17 different aerosol models can be selected. The wind, rain, cloud, visibility, and other meteorological inputs are entered as TAF code format. It is likely that future implementations of the EOTDA will automate the meteorological inputs. Automation will decrease the possibility of human error and will restore input data precision which was sacrificed for ease of use.

The operational input data are also entered in a user-friendly format. The sensor, target, and background configurations are selected from a data input screen. There are six backgrounds, 18 specific targets, several user-definable generic targets, and many sensors to choose from.

The run times range from a few seconds to several minutes, depending on the type of computer (e.g., 80486 vs. 80286), the target complexity, and the number of output times selected. Besides the numeric and graphical outputs, a visualization display is available that portrays the radiance values of the background and each target node pictorially.

## **FLEET USE OF THE EOTDA**

Infrared technology was employed extensively in the Persian Gulf during Operation Desert Storm, but the EOTDA was not widely used (Havener and Funk, 1991). When the EOTDA was used, it favorably influenced mission planning decisions. The desert background model proved

inaccurate early in the war, but this problem was corrected with a software fix. While some forecasts were found to be incorrect, the overall predictions were considered adequate. However, there was little feedback on the accuracy of the predictions, because the Desert Storm pilots and planners only required general (good, marginal, or poor) forecasts. The most difficult problem reported by meteorologists operating the EOTDA was not with the EOTDA itself, but getting accurate battlefield weather conditions and forecasts to input into the model.

Havener and Funk offer suggestions based on Desert Storm for improving the utility of the EOTDA. One was to tailor the output to the needs of the user. The level of detail required from the EOTDA varied with the type of mission. For example, an aircraft looking for targets of opportunity only needs general information on the IR conditions for various times of the day. For an aircraft striking a specific target, more detailed information on detection and lock-on ranges would help determine the best weaponry and strategies to minimize vulnerability. Version 3 of the EOTDA addresses this suggestion by allowing the user to specify the contents of the output. Other suggestions included: provide more training and awareness, automate the inputs, and provide a capability to correct and redefine the backgrounds and a capability to define new targets.

The EOTDA is more sophisticated and contains more capabilities than the UFLR model (Computer Sciences Corporation, 1986) residing in the current shipboard Tactical Environmental Support System. It is also much easier to use and has wider distribution than previous versions. Transitioning the EOTDA into TESS(3) will further increase the availability to the fleet. It is reasonable to assume that the fleet's use of the EOTDA will increase dramatically in the coming years. Therefore, it is crucial that the EOTDA be properly evaluated to determine the validity of its output and to identify any problem areas.

## VALIDATION OF THE EOTDA

Ideally, the limitations and accuracies of a TDA should be quantified so that the user can properly apply the information it provides. However, the complex modeling requirements and the numerous possibilities of environmental and physical parameters that define an optical scene make calibrating a TDA a formidable task for even a single sensor and target. The best that can be done in most cases is to verify the basic physics involved for each subroutine and then perform a variety of validation tests under whatever limited conditions naturally occur during the testing period. Much of the physics of the EOTDA is from well-accepted methodology, but little has been done to quantitatively validate the overall performance.

Sensitivity tests have been performed (e.g., Shapiro, 1989). However, sensitivity tests do not validate the model. Sensitivity tests vary the input parameters for a given base case to show how much each parameter affects the results for a given scenario. For example, small amounts of rain or battlefield-induced contaminants were shown to have a large effect on detection range (Keegan, 1990). In general, clouds were shown to reduce temperature contrast which tends to reduce detection range. However, Shapiro showed that the presence of clouds can actually improve detection range in some cases by delaying or preventing a temperature contrast reversal of the target against the background. While sensitivity tests are important for understanding the behavior of the model, they do not indicate absolute accuracy, and they only apply to the base case conditions.

Real-world validation tests cannot fully determine accuracy and variability either. However, it is important to measure TDA performance from an end-user perspective. A TDA that performs

well in theory but cannot be trusted in battle is dangerous. The result will be either poor mission planning or a TDA that will be ignored. End-to-end evaluations typically compare reports of detection ranges from air crews with the EOTDA predictions. Tests controlled by researchers are costly and large data samples over a wide range of conditions are usually unobtainable. Also, it is difficult to quantify the performance differences among different air crews and different aircraft. In spite of the difficulties, this type of evaluation is crucial in defining the usefulness and limitations of the TDA in real-world situations, and often identifies problems that go unnoticed in modular and theoretical testing.

NRL Monterey has conducted several evaluations in the past using measurements from aircraft out of naval air stations at Whidbey Island, Moffett Field, and Lemoore. Data from these measurements have led to TDA improvements and were used to compare various TDAs. These comparisons were instrumental in deciding to include the EOTDA Mark III into TESS(3). The aircraft measurements presented in this report advance the validation process and also illuminate some concerns that need to be investigated.

The primary data for this report stem from an IR experiment conducted 29 July to 4 August 1992 off the coast of Monterey, California, by NRaD in cooperation with the Naval Postgraduate School. The purpose of the experiment was to collect a comprehensive set of meteorological and ship temperature data for validation of the Performance and Range of Electro-Optical Systems (PREOS) detection range algorithm (McGrath, 1992) and the SHIPSIG thermal model for combatant ships (Ostrowski and Wilson, 1985; Ostrowski, 1993). The initial results of the PREOS validation were documented in a thesis for the Naval Postgraduate School (Kreitz, 1992). The SHIPSIG evaluation was combined with a comparison of TCM2 and presented in another NRaD report (McGrath, Jensen, and Ostrowski, 1994). The field data are further utilized in this report to evaluate the EOTDA Mark III.

## MEASUREMENTS

### OVERVIEW OF FIELD TESTS

A field experiment was conducted 29 July to 4 August 1992 using the Research Vessel *Point Sur* as the primary measurement platform. *Point Sur* is a 135-foot ship that is owned by the National Science Foundation. It served as a platform for meteorological and surface measurements and as an IR target for the airborne FLIR and imaging systems. Scientists from the Naval Postgraduate School, NRaD, and Naval Surface Warfare Center (NSWC) were aboard the *Point Sur* to conduct the onboard measurements. Figure 1 shows the ship track for the 5-day cruise as recorded by the Global Positioning System (GPS) receiver.

Air temperatures ranged from 11.5 to 17.8°C during the cruise. Sea temperatures were from 11.0 to 18.1°C, with a warmer sea than air temperature most of the time. Wind speeds ranged from 3 to 26 knots, and were predominately from the Northwest. Stratus clouds dominated until the last day of the test when clear skies prevailed. The stratus base ranged from 500 to 1300 feet according to the aircrew reports. Cloud tops as determined from radiosonde relative humidity gradients ranged from 1200 to 2100 feet.

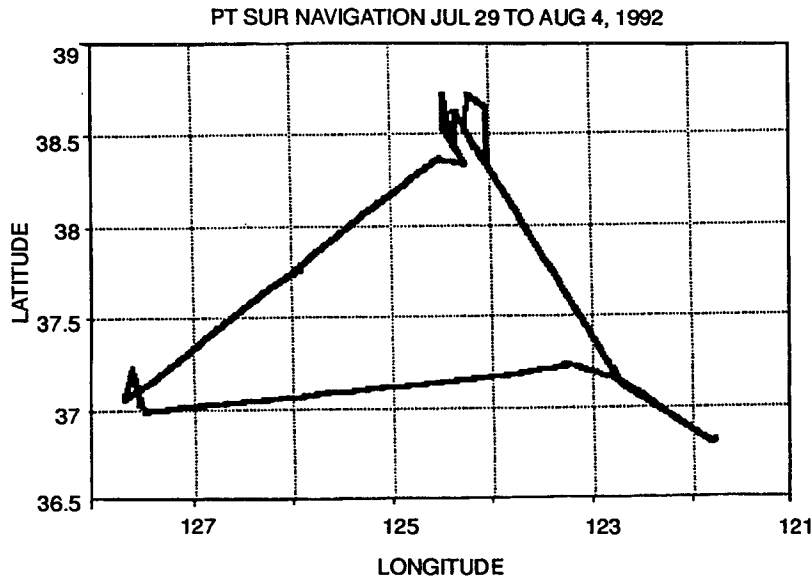


Figure 1. Research Vessel *Point Sur* GPS track.

## SHIPBOARD MEASUREMENTS

Ground-truth measurements of the skin temperatures of the ship were collected from 15 thermistors attached to the ship, and a hand-held radiometer. The thermistors were mounted on the large-area surfaces of the ship and were continuously recorded. Spot measurements of IR skin temperature were made several times daily with a hand-held radiometer that operated in the 8–12  $\mu\text{m}$  band.

Meteorological data were collected by the Naval Postgraduate School from a variety of shipboard sensors. The surface parameters measured included: air temperature, sea temperature, dewpoint temperature, wind speed, wind direction, relative humidity, pressure, and solar irradiance. Vertical profiles of meteorological parameters were obtained from a VAISALA RS80 rawinsonde system. The calibrated accuracies of this system are within 0.5 mb pressure, 0.2°C temperature, 2% relative humidity, and 2% altitude. Atmospheric radon concentrations were also recorded as an aid to identifying continental versus marine air masses. Among the ship navigation data recorded were latitude, longitude, gyro heading, and ship speed.

## AIRBORNE PLATFORM MEASUREMENTS

The NRaD airborne platform is a Piper Navajo aircraft that is outfitted with navigation, meteorological, aerosol and thermal image recording systems. The aircraft flew 11 missions. Meteorological and aerosol data were collected as a function of altitude in 13 spiral ascents, each beginning at 200 feet and climbing to 5000 feet. A total of 2603 image frames of the *Point Sur* were collected with the AGA-780 Radiometric Thermal Imaging System, which was operated in the 8–12  $\mu\text{m}$  band. Additional meteorological and aerosol data were collected at 200-foot and 500-foot altitudes during the image collections. Meteorological and navigational parameters were recorded at 5-second intervals. These included date, time, GPS latitude and longitude, altitude, air temperature, dewpoint temperature, relative humidity, and atmospheric pressure.

## AIRBORNE FLIR MEASUREMENTS

Aircraft employing an 8–12  $\mu\text{m}$  FLIR system with a mercury-cadmium-telluride (HgCdTe) sensor detector flew range detection missions during the field tests. Eight missions were flown, for a total of 57 FLIR target runs over a 5-day period. Two flights were scheduled per day, one at night about 0600 hours GMT (2300 PDT, 2200 PST) and the other in the morning at about 1700 hours GMT (1000 PDT, 0900 PST). Exact flight times are listed in the tables of Appendix A.

A representative from the Naval Postgraduate School instructed flight crews in a preflight briefing before each mission. The aircrews had voice and visual contact with the *Point Sur* before making detection runs. Runs were made from two altitudes: 500 and 1000 feet. For consistency, all detection ranges were determined using the wide ( $15 \times 20$  degree) field of view lens. Target classification and identification ranges were determined using the narrow ( $5 \times 6.7$  degree) field of view lens. Detection was defined as when the operator first notices a dot on the display. The aircrew operator recorded the detection ranges and requested supplemental information on data sheets provided for the tests. Display images were preserved on video tape, which is now archived at the Naval Postgraduate School.

## EOTDA OPERATION

The input values required to operate the EOTDA include meteorology, navigation, and operational parameters. Entering the operational parameters, such as type of sensor, aircraft altitude, and ship heading, is a straightforward transfer of measured values. In contrast, the meteorological parameters are more difficult to input because they require some interpretation. Visibility, for example, significantly affects detection range calculations, but is difficult to measure accurately. Wind direction and speed were measured continuously, but the precise values must be translated to TAF code to operate the EOTDA, which tends to degrade the precision.

Comparison tests at NRL Monterey noted discrepancies in the output between versions 2.0 and 3.0. When the meteorological input format was changed from the tabular format in version 2.0 to TAF code format in version 3.0, some software errors resulted. It is possible that some of the detection range error in this data set could be from program errors rather than model performance. However, this is unlikely. The TAF code input was checked for proper format, and the binary input files created by the EOTDA were spot checked to verify that the cloud and other meteorological data were actually getting into the program. Furthermore, the input values were from carefully monitored in-situ measurements, rather than imprecise forecasts. It is therefore reasonable to assume that the output results are primarily from model performance.

## RESULTS

### DETECTION RANGES

Figure 2 is a scatter plot of the detection ranges predicted by the EOTDA compared with the detection ranges observed by the aircrews. The same data are presented in tabular and bar graph form in Appendix A for each of the eight missions. The data show a tendency of the EOTDA to overpredict the detection ranges. There was no significant difference between the results of the morning flights compared with the night. An overcast stratus layer prevailed throughout the

testing period, except on 4 August, the final night of the field tests. The EOTDA predictions agree more closely with the observed detection ranges on the clear weather day, 4 August, but grossly overpredict the detection range during the stratus cloud conditions. At first glance, the EOTDA cloud model appears to need some refinements, but the problem is not that simple. A multitude of interrelated factors is involved. Sensitivity tests (Shapiro, 1989) show that clouds can greatly affect detection range, but the effects are maximum during the daylight hours and minimal at night. The field data show the error difference between the clear day and stratus days is large regardless of whether the overflight was night or morning. This suggests that there is more than simply cloud effects causing the overprediction of ranges.

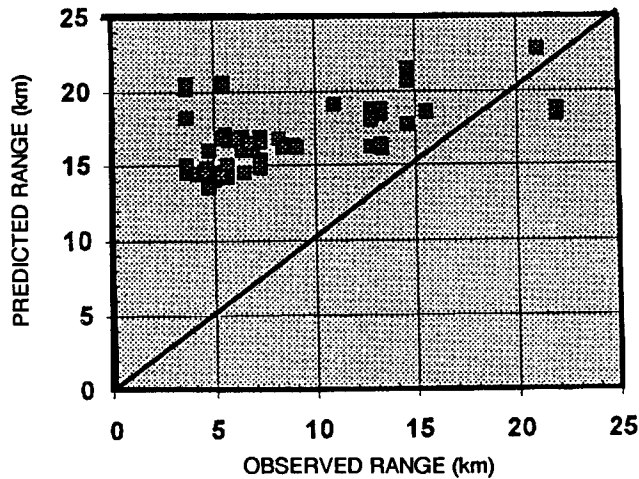


Figure 2. Observed detection ranges compared with EOTDA MDT range predictions.

## BACKGROUND TEMPERATURES

The tables in Appendix B tabulate the differences between the TDA-calculated background temperatures and the measured sea temperatures. Figures 3 and 4 use the data from these tables to compare the measured and calculated water background temperatures for each overflight. Figure 3 is a scatter plot of the temperature values. Figure 4 shows the magnitudes of the temperature differences for each set of flights (with zero being perfect agreement). The calculated values of the physical sea temperature are taken directly from the EOTDA output file FACET.TMP. The measured sea temperatures were taken aboard the *Point Sur* during the cruise from a thermistor submerged in the water. The thermistor measurement depth ranged from about 3 to 12 inches, depending on the ship speed. Radiometric sea temperatures were also measured from onboard the *Point Sur*. The radiometric values were taken with a hand-held 8–12  $\mu\text{m}$  Everest radiometer. Figure 5 shows that the onboard thermistor and radiometric temperatures are in close agreement. The onboard radiometric and thermistor sea temperatures ranged from 11.0 to 18.1°C over the entire test period, with an average agreement of 0.1°C and standard deviation of 0.3.

Figure 4 shows that the TDA calculations of the physical sea temperatures are within  $\pm 2.0^\circ\text{C}$  on the stratus weather days. On the clear sky day, the TDA overpredicted the physical sea temperature an average of 3.4°C. While the background temperature predictions showed the largest errors with the clear weather data, the range predictions were most accurate for this same data set. Part of the reason for this apparent contradiction is that the contribution of water emissivity

to total background radiance is minimized at large angles of incidence, as shown by Fresnel's equation plotted in figure 6 (Shapiro, 1987). The incidence angles for this data set ranged from 85.8 to 89.6 degrees, assuming a smooth ocean surface and isotropic radiation. Although the real-world sea surface is never perfectly smooth and some diffuse radiation is always present, the angles are such that reflected sky radiance makes a major background contribution.

The measurements indicate that the most significant errors in the background temperature predictions probably stem from the integrated sky radiance and ocean surface reflectance calculations. Unfortunately, validation of the sky contribution is not possible for this data set. The data did not include sky radiance measurements or simultaneous radiometric imaging of the target and background.

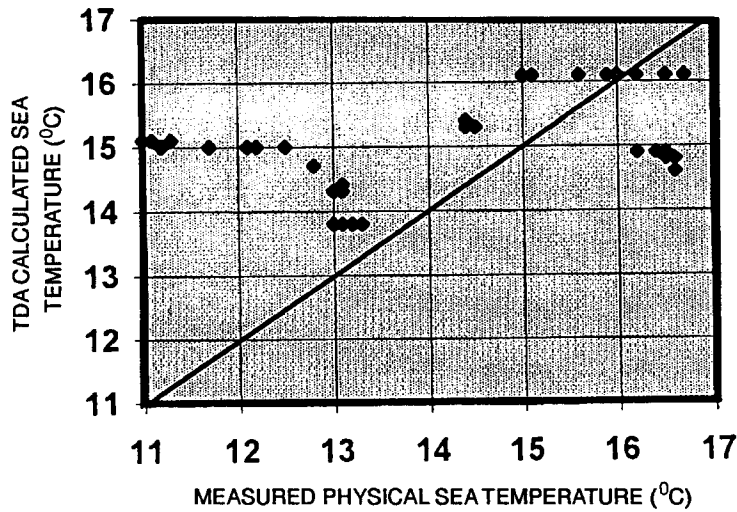


Figure 3. EOTDA calculated sea temperature compared with measured values.

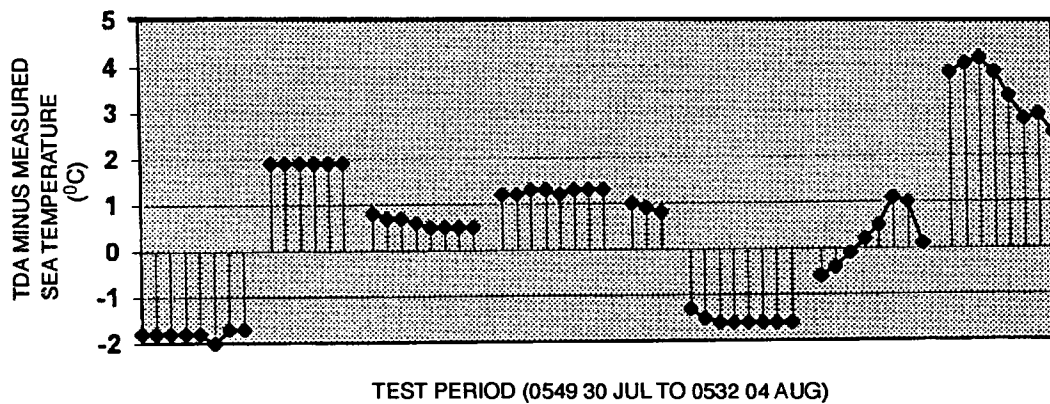


Figure 4. Background temperature differences over the test period (57 overflights); Point Sur thermistor values minus the EOTDA predicted values.

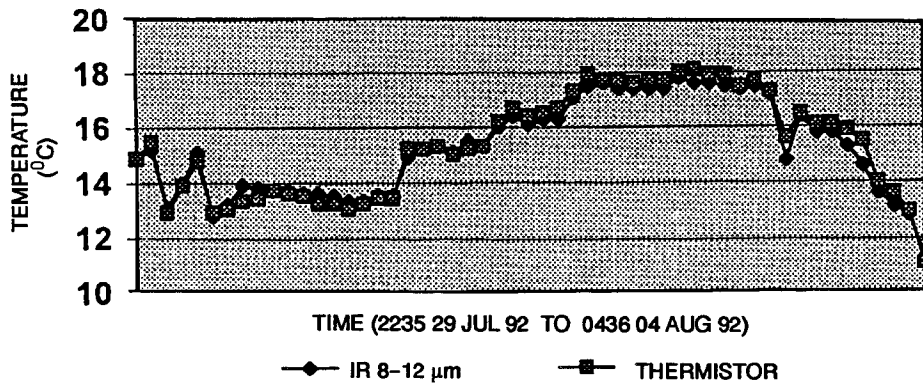


Figure 5. Comparison of radiometric and physical sea temperatures.

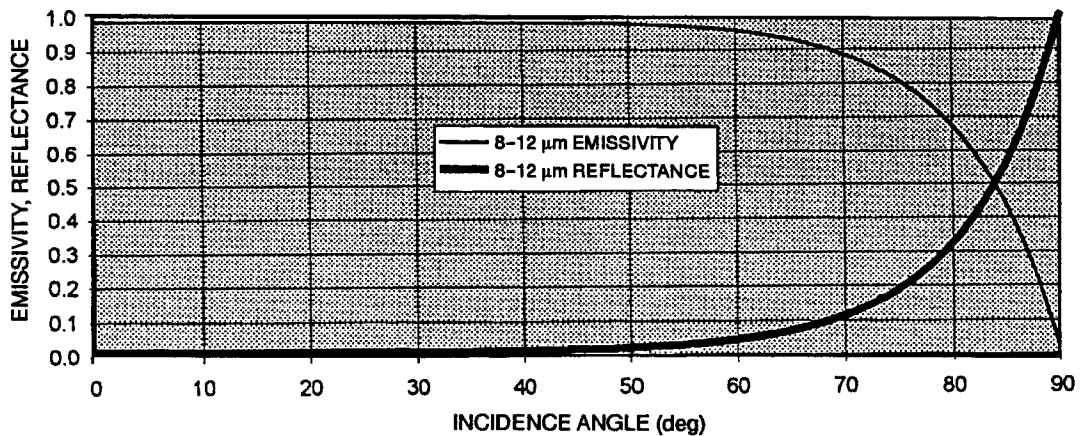


Figure 6. Emissivity and reflectance of sea water as a function of incidence angle.

## TARGET TEMPERATURES

The target temperatures predicted by the EOTDA are believed to be reasonably accurate for the data set presented here. Calibrated thermal images of the target were analyzed and the path effects were removed (Hughes and McGrath, 1993). These corrected values were compared to the Georgia Technology Research Institute program TCM2 and the NSWC program SHIPSIG (McGrath, Jensen, and Ostrowski, 1994). The model and target temperatures agreed within  $\pm 2.0^{\circ}\text{C}$ . Table 1 shows a set of the corrected AGA-780 thermal imager temperatures and the TDA target temperatures for the starboard and port views of the target. The overall average temperature of the TDA was  $15.3^{\circ}\text{C}$ , and the AGA-780 image temperature average was  $17.5^{\circ}\text{C}$ . This temperature difference is easily explained by time difference between the airborne AGA measurements and the aircraft FLIR measurements. All of the AGA measurements were made in the afternoon, when a hotter target is likely. The TDA validation measurements using the FLIR system were made late at night and at mid-morning when a cooler target temperature is expected. Thus, the 2.2 degree average temperature difference is not unreasonable. No simultaneous measurements were taken with operational FLIR and the AGA imager, so a direct correlation of measured and predicted temperatures is not possible. Attempts to correlate the FLIR and AGA with thermistor recordings of the target also proved unsuccessful. Twelve thermistors were attached to the target during the field experiment, but none of the individual thermistors

adequately tracked the average target temperatures. No scheme of combining the thermistor values has yet been devised that represents the composite ship temperature. Until a better data set is available, the target model cannot be properly validated. Meanwhile, it appears that the target model is functioning with an accuracy of  $\pm 2.0^{\circ}\text{C}$ .

Table 1. Comparison of target temperatures from the AGA-780 imager and the TDA predictions for the starboard and port sides.

Date	GMT	LOCAL	STB AGA	STB TDA	PRT AGA	PRT TDA
Jul 29	2230	3:30 PM	17.5		18.1	
Jul 30	0115	6:15 PM	15.3		16.0	
Jul 30	0610	11:10 PM		14.8		14.8
Jul 30	1715	10:15 AM		14.5		13.9
Jul 30	2045	1:45 PM	18.3		18.5	
Jul 31	0700	12:00 AM		15.2		15.1
Jul 31	1715	10:15 AM		17.5		17.1
Jul 31	2115	2:15 PM	19.1		19.0	
Aug 01	0510	10:10 PM		15.2		15.2
Aug 01	1745	10:45 AM		16.8		17.2
Aug 01	2030	1:30 PM	18.9		19.6	
Aug 03	1745	10:45 AM		17.1		16.6
Aug 03	1930	12:30 PM	18.3		17.0	
Aug 03	2230	3:30 PM	16.8		16.7	
Aug 04	0145	6:45 PM	16.1		15.2	
Aug 04	0500	10:00 PM		12.2		11.9

## CONCLUSIONS

Since the EOTDA program development was primarily directed toward Air Force applications, little has been done to test and validate the marine environment. The results presented here clearly show the need to further investigate and improve the EOTDA. The TDA performed well on the clear sky day of the tests and performed poorly on the stratus days. Tests should especially focus on the transmission, sky radiance, cloud, and water background models.

It is hoped the EOTDA operation can be fully automated in the future. By interfacing the EOTDA to a weather forecasting system, input reliability and consistency are attainable, and the program will be easier to use. It appears, however, that the TDA predictions are unreliable in some situations. Therefore, an experienced human operator is still required to interpret the results and adjust the predictions based on feedback from similar scenarios. For example, an operator who knows that the model overpredicts detection ranges in an open ocean background when there is a prevailing stratus cloud ceiling could introduce a correction factor (e.g., divide by 2.5) that would make the results more accurate. Hopefully, further validation and testing will provide solutions that do not require intervention.

The current EOTDA is a vast improvement over the UFLR program that is currently in TESS. The upgraded user-interface makes the program much easier to use, and the models push the limit of the original intended platform, a PC with a 80286 processor. The fleet use of the TDA should greatly increase now that the program is easier to use and has a wider distribution.

Inclusion into TESS(3) should further increase the usage of the EOTDA. It is therefore, critical that the model be more fully validated and any problems be annotated and corrected as quickly as possible.

## REFERENCES

- Blakeslee, L., and L.J. Rodriguez, "User's Manual for TCM2," Georgia Institute of Technology, Interim report for period Jan-June 1993 under Wright-Patterson AFB Contract F33615-88-1865 (July 1993).
- Computer Sciences Corporation, "Forward Looking Infrared Performance Function Program Performance Specification (PPS) for the Tactical Environmental Support System (TESS), Naval Ocean Systems Center Technical Document TD 1000 (December 1986).
- Freni, J. M. L., M. J. Gouveia, D. A. DeBenedictis, I. M. Halberstam, D. J. Hamann, P. F. Hilton, D. B. Hodges, D. M. Hoppes, J. J. Oberlatz, M. S. Odle, C. N. Touart, and S-L Tung, "Electro-Optical Tactical Decision Aid (EOTDA) User's Manual, Version 3," Phillips Laboratory Technical Report PL-TR-93-2002 Vol. I & II (11 January 1993).
- Havener, K., and S. Funk, "The Utility of Electro-Optical Tactical Decision Aids (EOTDAs)," USAF Air Weather Service Report No. AWS/XTA 91-1 (10 September 1991).
- Hughes, H. G., and C. P. McGrath, "Surface Ship Infrared Signatures Determined Using an Airborne Imaging System," Science and Technology Corporation Technical Report 2727 (September 1993).
- Keegan, T. J., "EOTDA Sensitivity Analysis," Air Force Geophysics Laboratory Technical Report No. GL-TR-90-0251 (II), (27 September 1990).
- Kneizys, F. X., E. P. Shettle, L. W. Abreu, J. H. Chetwynd, Jr., G. P. Anderson, W. O. Gallery, J. E. A. Selby, and S. A. Clough, "Users Guide to LOWTRAN 7," Air Force Geophysical Laboratory Technical Report No. 88-0177 (1988).
- Kreitz, J. C., "Preliminary Evaluation of the PREOS Program for Determining Detection Ranges of Airborne FLIR Systems," Naval Postgraduate School Thesis (December 1992).
- McGrath, C. P., "PREOS Program for Determining Detection Ranges of Airborne FLIR Systems," NRaD Technical Report 1488 (January 1992).
- McGrath, C. P., D. R. Jensen, and P. P. Ostrowski, "Surface Ship Infrared Signature Model Evaluation," NRaD Technical Report 1647 (April 1994).
- Ostrowski, P. P., and D. M. Wilson, "A Simplified Computer Code for Predicting Ship Infrared Signatures," Naval Surface Warfare Center Technical Report 84-540 (1985).
- Ostrowski, P. P., "A Simple Thermal Model for FLIR Detection Range Applications," meeting of IRIS Specialty Group on Targets, Backgrounds, and Discrimination, Vol II, pp 177-190 (July 1993).
- Shapiro, R., "Mark III Infrared Operational Tactical Decision Aids for Navy Operations: A Sensitivity Analysis," Naval Research Center Monterey California Contractor Report No. CR-89-12 (September 1989).
- \_\_\_\_\_. "Water Backgrounds in the Infrared (IR) and Visible (TV) Tactical Decision Aids," Air Force Geophysics Laboratory Report AFGL-TR-87-0254 (August 1987).

**Appendix A**  
**TABLES OF OBSERVED DETECTION RANGES AND EOTDA**  
**PREDICTIONS**

Jul 30 (GMT)	Altitude (ft)	Dpr Ang (deg)	Incidence Ang (deg)	Tgt Azm rel bow	Observed Rng (km)	Predicted Rng (km)	Difference Obs-TDA
0549	500	1.59	88.4	108	5.5	16.9	-11.4
0558	500	1.59	88.4	265	5.5	16.9	-11.4
0607	500	2.39	87.6	359	3.7	14.5	-10.8
0615	500	1.19	88.8	169	7.3	15.4	-8.1
0621	750	1.59	88.4	090	8.2	16.8	-8.6
0629	650	1.38	88.6	240	8.2	16.8	-8.6
0648	550	1.50	88.5	259	6.4	16.9	-10.5
0655	550	1.75	88.2	069	5.5	16.8	-11.3
Min	500	1.19	87.6	069	3.7	14.5	-11.4
Max	750	2.39	88.8	359	8.2	16.9	-8.1
Average					6.3	16.4	-10.1
Std Dev					1.6	0.9	1.4

Jul 30 (GMT)	Altitude (ft)	Dpr Ang (deg)	Incidence Ang (deg)	Tgt Azm rel bow	Observed Rng (km)	Predicted Rng (km)	Difference Obs-TDA
1702	350	1.11	88.9	105	5.5	20.6	-15.1
1708	300	1.43	88.6	302	3.7	20.2	-16.5
1714	500	2.39	87.6	082	3.7	20.5	-16.8
1719	300	0.95	89.0	278	5.5	20.4	-14.9
1727	500	2.39	87.6	162	3.7	18.2	-14.5
1733	500	1.19	88.8	354	7.3	16.9	-9.6
Min	300	0.95	87.6	082	3.7	16.9	-16.8
Max	500	2.39	89.0	354	7.3	20.6	-9.6
Average					4.9	19.5	-14.6
Std Dev					1.5	1.5	2.6

Jul 31 (GMT)	Altitude (ft)	Dpr Ang (deg)	Incidence Ang (deg)	Tgt Azm rel bow	Observed Rng (km)	Predicted Rng (km)	Difference Obs-TDA
0645	500	1.35	88.7	185	6.5	14.5	-8.0
0652	500	1.36	88.6	107	6.4	16.0	-9.6
0700	500	1.26	88.7	251	6.9	16.0	-9.1
0706	500	1.65	88.4	008	5.3	14.5	-9.2
0711	800	1.91	88.1	152	7.3	14.8	-7.5
0717	800	2.78	87.2	009	5.0	14.0	-9.0
0725	800	3.00	87.0	129	4.7	14.8	-10.1
0731	800	3.82	86.2	318	3.7	15.0	-11.3
Min	500	1.26	86.2	008	3.7	14.0	-11.3
Max	800	3.82	88.7	318	7.3	16.0	-7.5
Average					5.7	15.0	-9.2
Std Dev					1.3	0.7	1.2

Jul 31 (GMT)	Altitude (ft)	Dpr Ang (deg)	Incidence Ang (deg)	Tgt Azm rel bow	Observed Rng (km)	Predicted Rng (km)	Difference Obs-TDA
1706	438	1.37	88.6	287	5.6	17.1	-11.5
1712	438	1.42	88.6	134	5.4	16.8	-11.4
1720	444	1.37	88.6	178	5.7	15.0	-9.3
1726	444	1.35	88.7	331	5.8	16.7	-10.9
1736	674	1.61	88.4	096	7.3	16.6	-9.3
1743	675	1.32	88.7	303	9.0	16.4	-7.4
1750	673	1.29	88.7	026	9.1	16.2	-7.1
1756	676	0.92	89.1	206	12.8	16.2	-3.4
Min	438	0.92	88.4	026	5.4	15.0	-11.5
Max	676	1.61	89.1	331	12.8	17.1	-3.4
Average					7.6	16.4	-8.8
Std Dev					2.6	0.6	2.8

Aug 01 (GMT)	Altitude (ft)	Dpr Ang (deg)	Incidence Ang (deg)	Tgt Azm rel bow	Observed Rng (km)	Predicted Rng (km)	Difference Obs-TDA
0505	800	1.05	89.0	248	13.4	16.1	-2.7
0513	548	1.13	88.9	110	8.4	16.2	-7.8
0520	538	0.72	89.3	316	13.1	16.2	-3.1
Min	538	0.72	88.9	110	8.4	16.1	-7.8
Max	800	1.13	89.3	316	13.4	16.2	-2.7
Average					11.6	16.2	-4.5
Std Dev					2.8	0.1	2.8

Aug 01 (GMT)	Altitude (ft)	Dpr Ang (deg)	Incidence Ang (deg)	Tgt Azm rel bow	Observed Rng (km)	Predicted Rng (km)	Difference Obs-TDA
1721	1000	1.36	88.6	137	12.8	18.8	-6.0
1734	1000	1.36	88.6	319	12.8	18.6	-5.8
1738	1000	1.36	88.6	148	12.8	18.1	-5.3
1742	1000	1.59	88.4	293	11.0	19.1	-8.1
1748	500	0.66	89.3	190	13.3	16.4	-3.1
1755	500	0.60	89.4	332	14.6	17.7	-3.1
1801	500	0.66	89.3	238	13.3	18.8	-5.5
1809	500	0.66	89.3	081	13.3	18.4	-5.1
Min	500	0.60	88.4	081	11.0	16.4	-8.1
Max	1000	1.59	89.4	332	14.6	19.1	-3.1
Average					13.0	18.2	-5.3
Std Dev					1.0	0.9	1.6

Aug 03 (GMT)	Altitude (ft)	Dpr Ang (deg)	Incidence Ang (deg)	Tgt Azm rel bow	Observed Rng (km)	Predicted Rng (km)	Difference Obs-TDA
1700	1000	3.68	86.3	297	4.8	13.5	-8.7
1710	1000	3.08	86.9	049	5.7	14.2	-8.5
1717	1000	3.27	86.7	014	5.3	14.3	-9.0
1725	1000	4.16	85.8	170	4.2	14.4	-10.2
1732	500	1.83	88.2	298	4.8	16.0	-11.2
1738	500	1.28	88.7	095	6.8	16.5	-9.7
1745	500	1.91	88.1	359	4.6	14.5	-9.9
1754	500	1.43	88.6	280	6.1	16.8	-10.7
Min	500	1.28	85.8	014	4.2	13.5	-11.2
Max	1000	4.16	88.7	359	6.8	16.8	-8.5
Average					5.3	15.0	-9.7
Std Dev					0.9	1.2	1.0

Aug 04 (GMT)	Altitude (ft)	Dpr Ang (deg)	Incidence Ang (deg)	Tgt Azm rel bow	Observed Rng (km)	Predicted Rng (km)	Difference Obs-TDA
0411	1027	0.85	89.1	101	21.0	22.8	-1.8
0425	1008	1.20	88.8	049	14.6	21.5	-6.9
0432	1020	1.39	88.6	184	12.8	18.0	-5.2
0441	1013	1.21	88.8	038	14.6	20.7	-6.1
0449	457	0.36	89.6	086	21.9	18.8	3.1
0503	508	0.57	89.4	083	15.5	18.6	-3.1
0511	538	0.43	89.6	267	21.9	18.4	3.5
0522	530	0.60	89.4	080	15.5	18.5	-3.0
Min	457	0.36	88.6	038	12.8	18.0	-6.9
Max	1027	1.39	89.6	267	21.9	22.8	3.5
Average					17.3	19.7	-2.4
Std Dev					3.7	1.8	3.9

Stratus	Altitude (ft)	Dpr Ang (deg)	Incidence Ang (deg)	Tgt Azm rel bow	Observed Rng (km)	Predicted Rng (km)	Difference Obs-TDA
Totals							
Min	300	0.60	85.8	008	3.7	13.5	-16.8
Max	1000	4.16	89.4	359	14.6	20.6	-2.7
Avg	622	1.67	88.3	195	7.5	16.6	-9.1
STDEV	207	0.83	0.8	105	3.3	1.8	3.3

Overall	Altitude (ft)	Dpr Ang (deg)	Incidence Ang (deg)	Tgt Azm rel bow	Observed Rng (km)	Predicted Rng (km)	Difference Obs-TDA
Totals							
Min	300	0.36	85.8	008	3.7	13.5	-16.8
Max	1027	4.16	89.6	359	21.9	22.8	3.5
Avg	642	1.55	88.4	183	8.9	17.0	-8.2
STDEV	220	0.84	0.8	105	4.8	2.1	4.1

**Appendix B**  
**TABLES OF MEASURED SEA TEMPERATURES**  
**AND EOTDA PREDICTIONS**

Jul 30 (GMT)	TDA Sky (deg C)	TDA Bkg Apparent	TDA Bkg Physical	Meas (deg C)	Difference TDA-Meas
0549	-10.7	4.8	14.8	16.6	-1.8
0558	-10.7	4.8	14.8	16.6	-1.8
0607	-10.7	4.8	14.8	16.6	-1.8
0615	-10.7	4.8	14.8	16.6	-1.8
0621	-10.7	5.3	14.8	16.6	-1.8
0629	-10.7	5.1	14.6	16.6	-2.0
0648	-10.7	4.9	14.8	16.5	-1.7
0655	-10.7	4.9	14.8	16.5	-1.7
Average	-10.7	4.9	14.8	16.6	-1.8
Std Dev	0.0	0.2	0.1	0.0	0.1

Jul 30 (GMT)	TDA Sky (deg C)	TDA Bkg Apparent	TDA Bkg Physical	Meas (deg C)	Difference TDA-Meas
1702	-14.3	1.8	14.7	12.8	1.9
1708	-14.3	1.7	14.7	12.8	1.9
1714	-14.3	2.1	14.7	12.8	1.9
1719	-14.3	1.7	14.7	12.8	1.9
1727	-14.3	2.1	14.7	12.8	1.9
1733	-14.3	2.1	14.7	12.8	1.9
Average	-14.3	1.9	14.7	12.8	1.9
Std Dev	0.0	0.2	0.0	0.0	0.0

Jul 31 (GMT)	TDA Sky (deg C)	TDA Bkg Apparent	TDA Bkg Physical	Meas (deg C)	Difference TDA-Meas
0645	-8.6	5.3	13.8	13.0	0.8
0652	-8.6	5.3	13.8	13.1	0.7
0700	-8.6	5.3	13.8	13.1	0.7
0706	-8.6	5.3	13.8	13.2	0.6
0711	-8.6	5.8	13.8	13.3	0.5
0717	-8.6	5.8	13.8	13.3	0.5
0725	-8.6	5.8	13.8	13.3	0.5
0731	-8.6	5.8	13.8	13.3	0.5
Average	-8.6	5.6	13.8	13.2	0.6
Std Dev	0.0	0.3	0.0	0.1	0.1

Jul 31	TDA Sky	TDA Bkg	TDA Bkg	Meas	Difference
(GMT)	(deg C)	Apparent	Physical	(deg C)	TDA-Meas
1706	-8.6	4.9	14.3	13.1	1.2
1712	-8.6	4.9	14.3	13.1	1.2
1720	-8.6	4.9	14.3	13.0	1.3
1726	-8.6	4.9	14.3	13.0	1.3
1736	-8.6	5.3	14.3	13.1	1.2
1743	-8.6	5.3	14.4	13.1	1.3
1750	-8.6	5.3	14.4	13.1	1.3
1756	-8.6	5.3	14.4	13.1	1.3
Average	-8.6	5.1	14.3	13.1	1.3
Std Dev	0.0	0.2	0.1	0.0	0.1

Aug 01	TDA Sky	TDA Bkg	TDA Bkg	Meas	Difference
(GMT)	(deg C)	Apparent	Physical	(deg C)	TDA-Meas
0505	-10.6	7.2	15.4	14.4	1.0
0513	-10.6	6.8	15.3	14.4	0.9
0520	-10.6	6.8	15.3	14.5	0.8
Average	-10.6	6.9	15.3	14.4	0.9
Std Dev	0.0	0.2	0.1	0.1	0.1

Aug 01	TDA Sky	TDA Bkg	TDA Bkg	Meas	Difference
(GMT)	(deg C)	Apparent	Physical	(deg C)	TDA-Meas
1721	-12.5	5.6	14.9	16.2	-1.3
1734	-12.4	5.6	14.9	16.4	-1.5
1738	-12.0	5.8	14.9	16.5	-1.6
1742	-12.0	5.8	14.9	16.5	-1.6
1748	-12.0	4.8	14.9	16.5	-1.6
1755	-11.7	5.0	14.9	16.5	-1.6
1801	-11.5	4.9	14.9	16.5	-1.6
1809	-11.2	5.1	14.9	16.5	-1.6
Average	-11.9	5.3	14.9	16.5	-1.6
Std Dev	0.4	0.4	0.0	0.1	0.1

Aug 03	TDA Sky	TDA Bkg	TDA Bkg	Meas	Difference
(GMT)	(deg C)	Apparent	Physical	(deg C)	TDA-Meas
1700	-10.6	9.2	16.1	16.7	-0.6
1710	-10.6	9.2	16.1	16.5	-0.4
1717	-10.6	9.2	16.1	16.2	-0.1
1725	-10.6	9.0	16.1	15.9	0.2
1732	-10.6	8.3	16.1	15.6	0.5
1738	-10.9	8.2	16.1	15.0	1.1
1745	-11.1	8.2	16.1	15.1	1.0
1754	-11.5	8.1	16.1	16.0	0.1
Average	-10.8	8.7	16.1	15.9	0.2
Std Dev	0.3	0.5	0.0	0.6	0.6

Aug 04	TDA Sky	TDA Bkg	TDA Bkg	Meas	Difference
(GMT)	(deg C)	Apparent	Physical	(deg C)	TDA-Meas
0411	-33.0	1.3	15.1	11.3	3.8
0425	-33.0	1.3	15.1	11.1	4.0
0432	-33.0	1.3	15.1	11.0	4.1
0441	-33.1	1.3	15.0	11.2	3.8
0449	-33.1	-0.4	15.0	11.7	3.3
0503	-33.1	-0.3	15.0	12.2	2.8
0511	-33.1	-0.3	15.0	12.1	2.9
0522	-33.1	-0.3	15.0	12.5	2.5
Average	-33.1	0.5	15.0	11.6	3.4
Std Dev	0.1	0.9	0.1	0.6	0.6

Stratus	TDA Sky	TDA Bkg	TDA Bkg	Meas	Difference
Totals	(deg C)	Apparent	Physical	(deg C)	TDA-Meas
Min	-14.3	1.7	13.8	12.8	-2.0
Max	-8.6	9.2	16.1	16.7	1.9
Avg	-10.7	5.5	14.8	14.7	0.1
STDEV	1.8	1.9	0.7	1.6	1.4

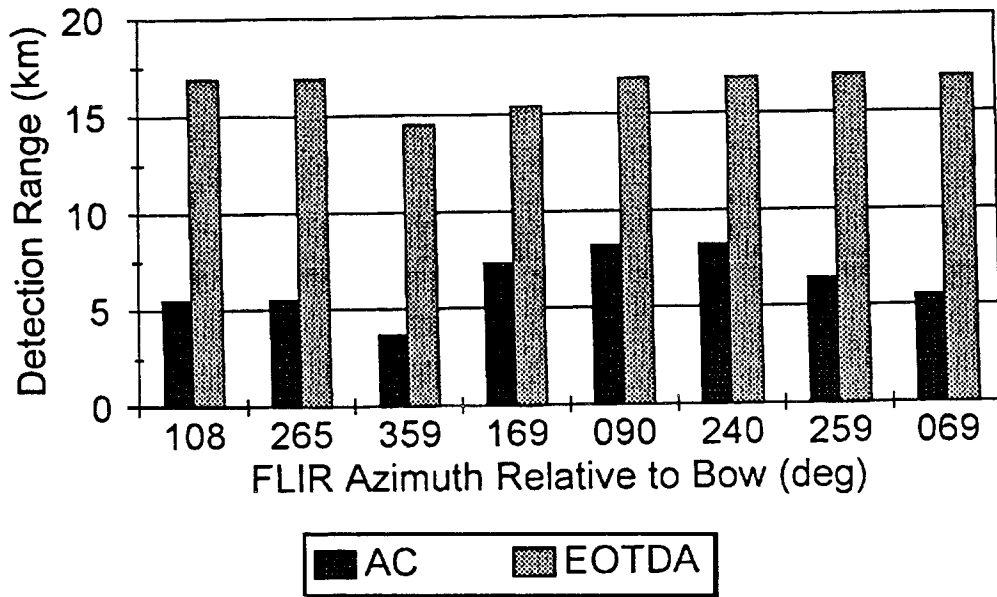
Overall	TDA Sky	TDA Bkg	TDA Bkg	Meas	Difference
Statistics	(deg C)	Apparent	Physical	(deg C)	TDA-Meas
Min	-33.1	-0.4	13.8	11.0	-2.0
Max	-8.6	9.2	16.1	16.7	4.1
Avg	-13.8	4.8	14.8	14.3	0.5
STDEV	8.0	2.5	0.7	1.9	1.7

Appendix C

BAR CHARTS OF OBSERVED AND PREDICTED DETECTION RANGES

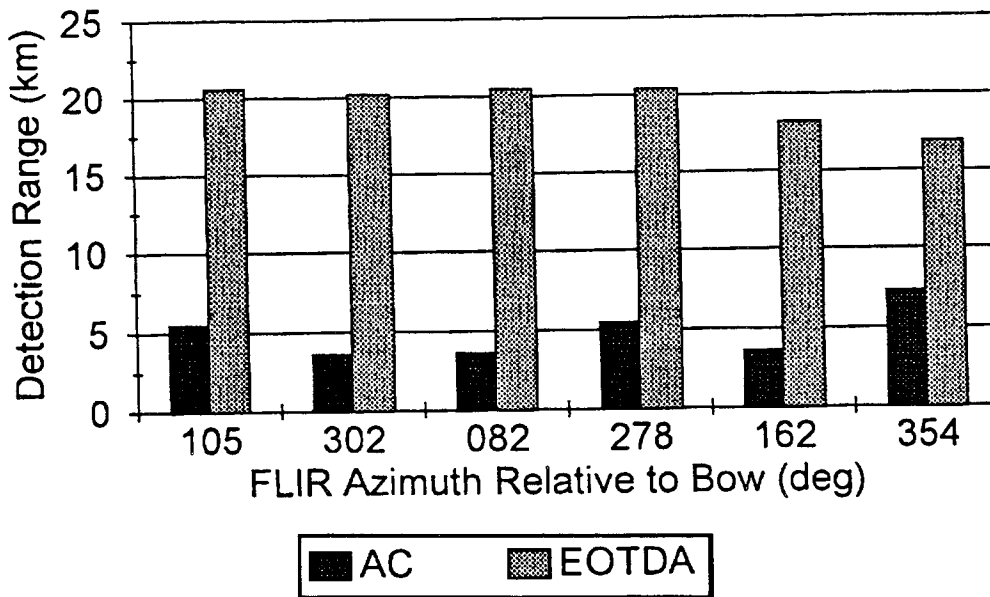
### Observed v. Predicted Range

30 Jul 0549 GMT, Stratus 1000 ft.



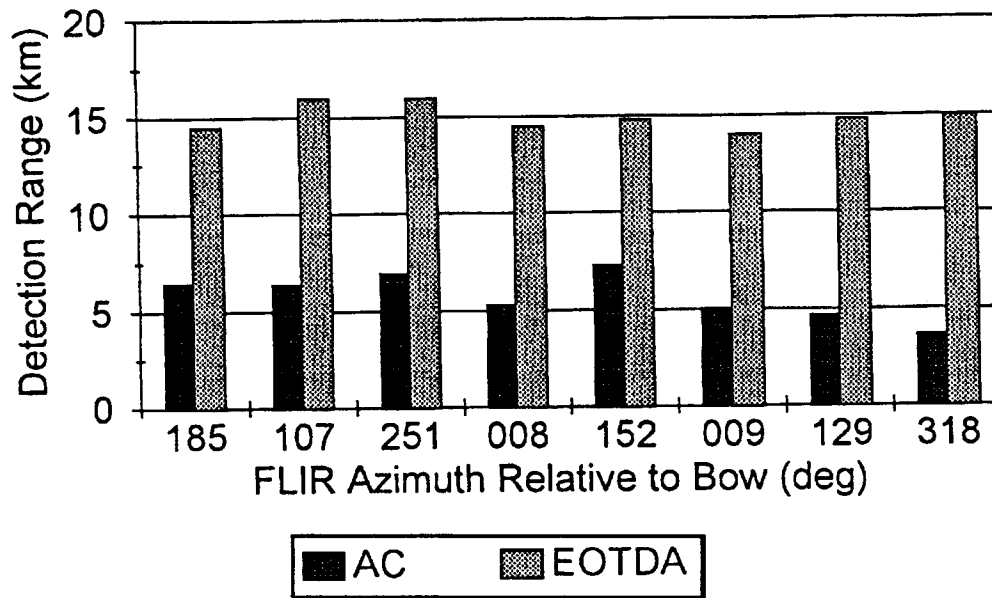
### Observed v. Predicted Range

30 Jul 1702 GMT, Stratus 800 ft.



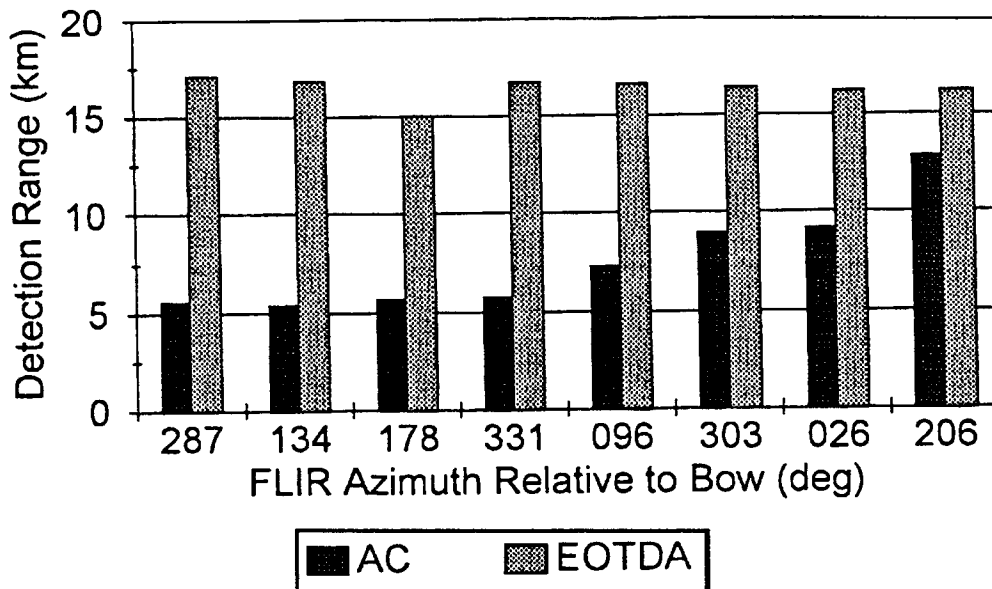
# Observed v. Predicted Range

31 Jul 0645 GMT, Stratus 850 ft.



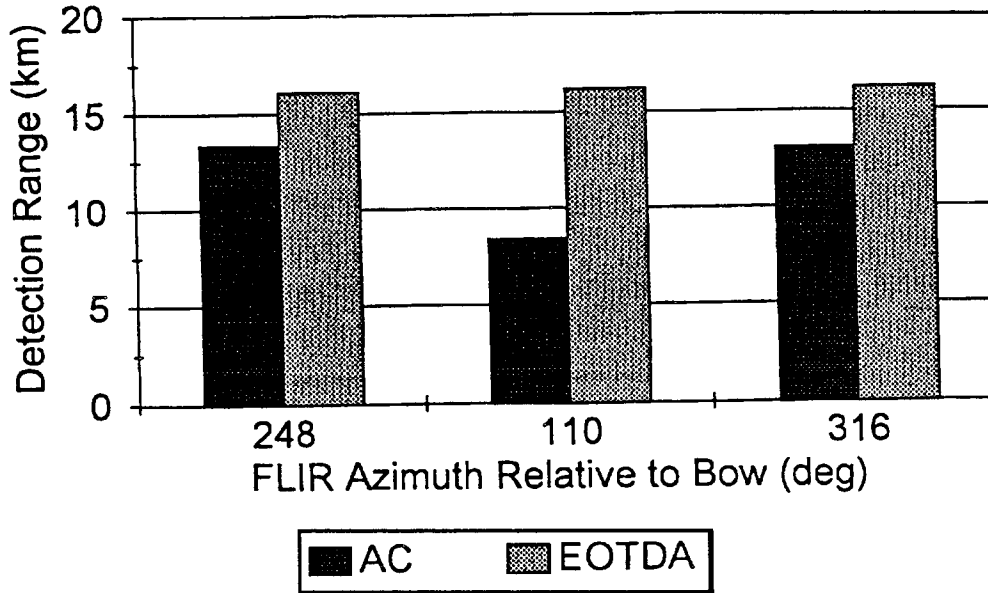
# Observed v. Predicted Range

31 Jul 1706 GMT, Stratus 700 ft.



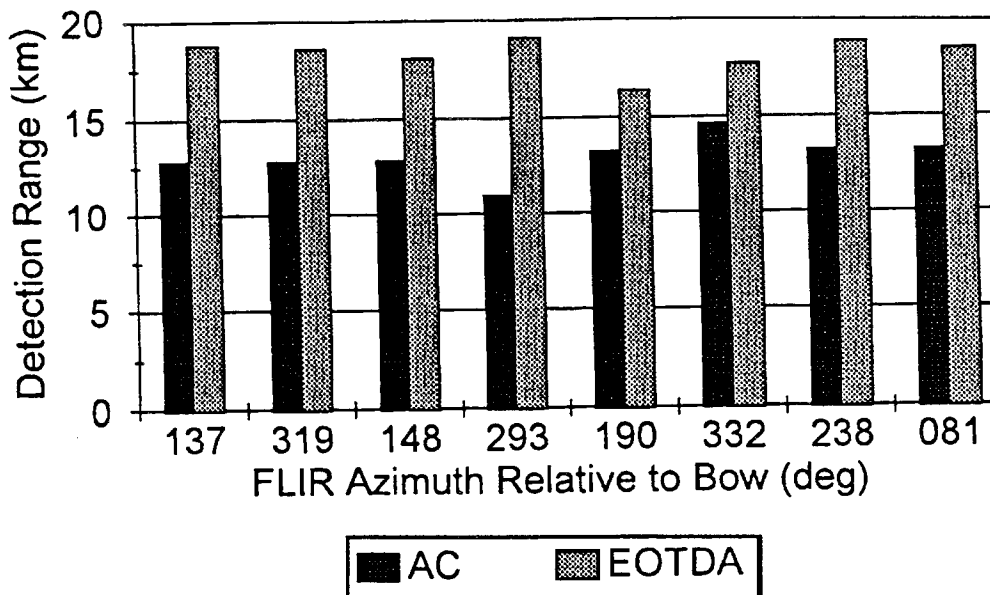
# Observed v. Predicted Ranges

1 Aug 0505 GMT, Stratus 1200 ft.



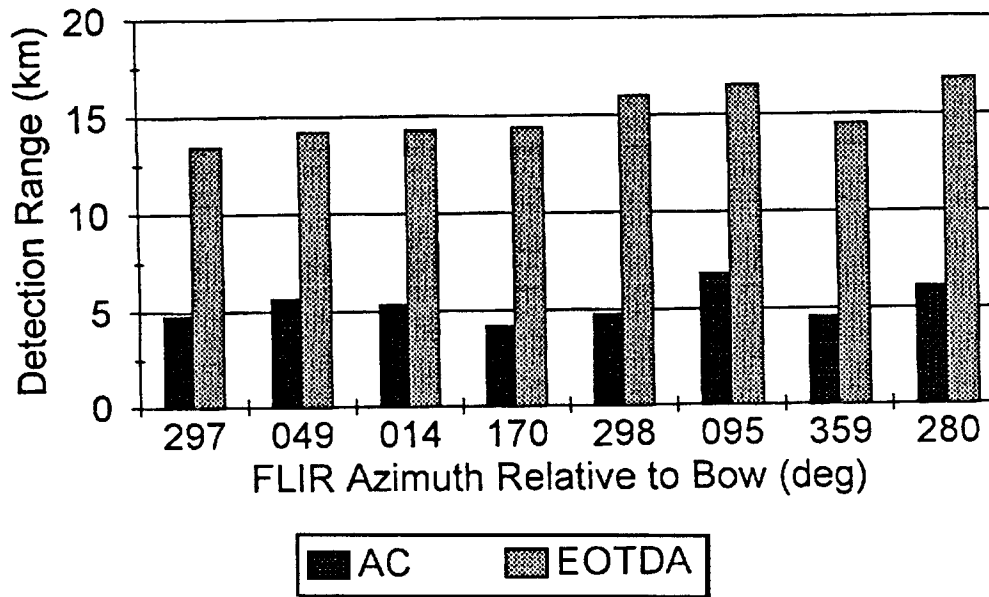
# Observed v. Predicted Ranges

1 Aug 1721 GMT, Stratus 1400 ft.



# Observed v. Predicted Ranges

3 Aug 1700 GMT, Stratus 1300 ft.



# Observed v. Predicted Ranges

4 Aug 0411 GMT, Clear Weather

